Effects of Ostia Variation for Airflow Patterns within Nasal Cavity Models with Maxillary Sinus

E. Afiza
Course of Science and Technology, Tokai University, Kanagawa, Japan
Email: ernyafiza@yahoo.com

Y. Takakura [1], T. Atsumi [2], and M. Iida [2]
[1] Course of Science and Technology, Tokai University, Kanagawa, Japan
[2] School of Medicine, Tokai University, Kanagawa, Japan
Email: takakura@tokai-u.jp

***Abstract*—In this study, the airflow is numerically simulated within models of human nasal cavity on the effect of the variation of ostia for the maxillary sinus. Four models were generated according to variation on the number of the ostia and also its position. As the results of flow patterns within the main nasal cavity, almost no significant difference can be observed with or without the maxillary sinus. Regarding flows in ostia and the maxillary sinus, changes appear: In the standard model (with an anterior ostium only), the mass flow rate during inhalation is significantly higher in comparison to that during exhalation. The mass flow rate entering the sinus can be increased with the presence of multiple ostia as the flow enters and exits at different ostia. On the other hand in the model with a posterior ostium only, the mass flow rate is almost same at inhalation and exhalation.**

***Index Terms*—numerical simulation, unsteady flow**

I. Introduction

Paranasal sinuses are paired air-filled spaces, and the certain reason for their existence, in fact, remains unclear except for reduction of weight in skull. The maxillary sinus is the largest among four groups for human paranasal sinuses. It is generally stated that the presence of maxillary sinus can be related to humidification of the inhaled air, voice enhancement, and also as shock absorber in trauma. The pyramid-shaped space with averaged capacity of 10-15ml are located below the cheeks, above the teeth and on the side of nasal cavity lined by mucosal membrane. The shape, size and location of maxillary sinuses vary significantly not only between individuals, but also between each sides of the same person. They are connected to media meatus through single or multiple opening called ostium/ostia. These openings (ostia) are situated near the top of the maxillary sinus, which may cause difficulties in draining its contents to the nasal cavity by gravity. On the side of the main nasal cavity, the ostia are located mostly in the anterior/middle region of the middle meatus.

The number of ostia is said to be one about more than half of healthy persons. However, in actual, it is unclear as it is difficult to visualize them directly from the middle meatus. It is stated that cadaver models possess higher rates of having more than one ostium compared to in vivo models [1], [2]. The reason might be that the mucosal tissue shrinkage during the measurement process makes the ostium more apparent. R Aust, *et al.* has established a method for measuring the functional size of ostia in vivo on the basis of pressure rise [3]. It is stated that, the average of the ostia diameters was 2.4mm among 37 subjects and there is almost no significant difference in the volume of the maxillary sinus and the diameter of the ostium between men and women. Ho-yeol Jang, et al. performed a study regarding the changes in ostia diameter as a consequence from elevating the sinus floor through surgery [4]. Their findings showed that the diameters of ostia are significantly decreased with the elevation of the sinus floor, which caused sinus obstructions.

Obstruction in sinus causes reduction in sinus ventilation and drainage, which can increase the possibilities of having maxillary sinus-related diseases such as sinusitis, for example, clogging of the ostia, septal deviation, swelling of the membrane tissue and many more [5]. Up until now, surgical operation in sinusitis is in attempt to increase the ventilation of the sinus. If accurate information related to the variation of the ostia is obtained on the airflow pattern in real model of the nasal cavity including the human maxillary, it can greatly contribute the medical treatment.

In vivo experiment is regarded to be most actual in visualizing the airflow pattern. However, direct measurements in the human nasal cavity are almost impossible due to the complexity of the geometry: crooked bends and narrowness. For example, as an intrusive method, the capability of direct visualization technique such as hot wire anemometry is restrained considering the obstruction effect to the airflow itself and the biological reaction against physical contact [6]. On the contrary, numerical simulation is advantageous in treating complex geometry.

Manuscript received December 30, 2014; revised July 3, 2015.

doi: 10.18178/jomb.5.2.98-102

While there are many papers about flows within main nasal cavities, researches on ventilation of sinuses are very few. C. M. Hood, et al. investigated the gas exchange in human maxillary sinus on the variation of the ostia length and diameter numerically by using very simple geometries and confirmed that the presence of multiple ostia causes a rise in mass flow rate followed by ventilation rate increment [7]. In the present research, by use of real-geometric models of a human nasal cavity including the maxillary sinus, the sinus ventilation is numerically investigated with purpose to clarify the morphologic role of the ostia to the maxillary sinus. Numerical experiments have been carried out about four types models generated according to presence or non-presence of the maxillary sinus, number and location of the ostia, and the changes have been investigated in the airflow pattern within the nasal cavity, maxillary sinus, and ostia.

II. Generation of Models and Grids

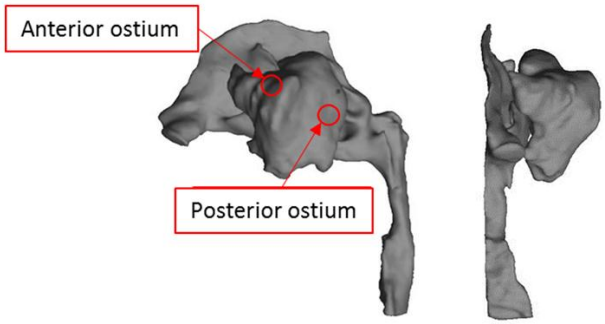

Figure 1. Maxillary sinus (front and side view)

By collaboration with Tokai University Hospital, a highly detailed configuration model of the human nasal cavity was fabricated as shown in Fig. 1. The three-dimensional nasal cavity model was reconstructed from a Computer Tomographic scan (CT scan) with spatial resolution 512x512 pixels, obtained by 0.3mm slice width. Only one of the two nasal cavities was studied considering that the anatomy of the nasal cavities is almost identical. A few features were disregard in this model: (a) nostril hairs, (b) external nose shape, and (c) properties of nasal tissues such as, moist and warm condition within the nasal cavity. The data was then imported into 3D slicer for volume rendering. It is a free source software and has been widely used particularly in medical purposes. Next, 3Ds Max Design was used to modify the 3D model of nasal cavity which includes deleting the unwanted features such as tongue, ethmoid sinuses, frontal sinus and many more. Feature variations that include the number of ostia and smoothing process were also performed by using the same software. The modified model was imported to ICEM CFD by using STL data to generate the mesh consisting tetra elements in the body and prism elements near the wall before the airflow pattern was simulated in Fluent. Four types of human nasal cavity models with and without the presence of maxillary sinus (volume: 20.6ml) were created as shown below:

(a) Model A : without the presence of maxillary sinus
(b) Model B : with the presence of anterior and posterior ostia
(c) Model C : with the presence of anterior ostium only (Standard Model)
(d) Model D : with the presence of posterior ostium only

The anterior ostium is located in the anterior/middle side of middle meatus. Meanwhile, the posterior ostium is in the vicinity of the posterior side of middle meatus. Model C represents the standard model with the presence of anterior ostia only which appears in more than half of healthy person [7].

III. Computational Condition

Reynolds number of airflow is 880, which is obtained from the average hydraulic diameter of nares of the model at maximum breathing rate [8]. Airflows for incompressible fluid are computed using FLUENT under the following boundary conditions: (1) The nasal wall is rigid with non-slip condition; (2) To mimic a natural breathing airflow, user defined function is utilized to simulate unsteady condition where the maximum flow velocity of 1.9m/s is given at the nasopharynx area. Periodic cycles for breathing start with the steady-state flow data at maximum inhalation and followed by exhalation, with period time of 3 seconds in each cycle. Simulation was performed for 3 cycles (9000 time-steps), achieving a converged solution at each time-step. The third cycle was evaluated as solution during one period.

IV. Grid Convergence

In order to obtain more accurate results without dependency of mesh size, before moving onto the simulation, grid convergence was investigated where the mesh is refined until the solution for the specified variable is converged to values independent on mesh size. By changing the global element factor of ICEM CFD, in Model B, seven types of grids with different mesh size were generated with 0.1 million cells being the coarsest and 2.4 million cells being the finest. Mesh in the ostia regions was set to the ratio of 90% smaller than the global element size in all types of grids to ensure more detailed results in the particular area.

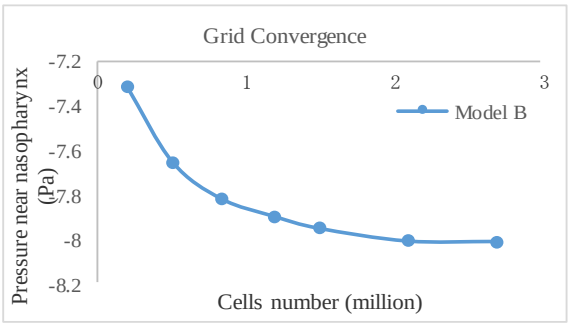

Figure 2. Grid convergence

For the steady solution of inspiration the pressure values at a point defined near the nasopharynx area are compared among all grids. As shown in Fig. 2, the grid resolution was converged as the grid approached 2.1 million cells with only 0.05% pressure difference with grid of 2.4 million cells. To save computing time and memory, the grid with 2.1 million cells was chosen to be the standard one throughout the present study.

V. Computational Results

A. Without Maxillary Sinus

Numerical results in model of the nasal cavity without maxillary sinus are presented in streamlines at peak inspiration and expiration in Fig. 3. During inspiration, the highest velocity distribution in the nasal cavity was recorded along the media meatus. A fairly large swirl was detected near the olfactory region in the superior meatus. Moreover, reversed-like flow was also found in the inferior meatus before entering the nasopharynx. Meanwhile during expiration, the mainstream is located along media and inferior meatus. A small-scale swirl was observed at the inferior meatus at the posterior side of the cavity.

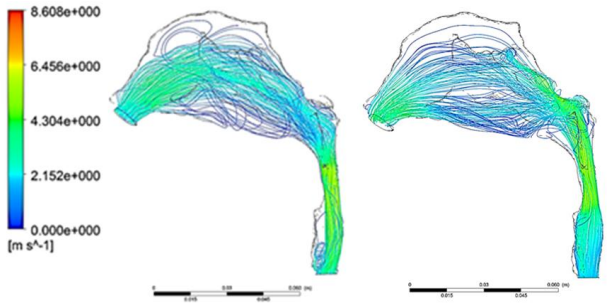

Figure 3. Streamlines in Model A (Without sinus) at peak inspiration (left) and expiration (right)

Almost no discrepancy can be observed in airflow patterns within the main nasal cavity between Model A and models with maxillary sinus (Models B, C and D).

B. Presence of Both Ostia (Anterior and Posterior)

Streamlines within the sinus at peak inspiration and expiration is shown in Fig. 4. The flow is unevenly distributed during inspiration as the flow focused at the anterior side of the sinus, while the flow circulated almost uniformly around the sinus during expiration,

Fig. 5 shows the velocity vectors in anterior and posterior ostia at peak inspiration. During inspiration, generally, the flow was introduced to the sinus through the anterior ostium, and exits at the posterior ostium.

TABLE I. Flow Results in Model B

	Peak inhale	Peak exhale
Mass flow rate (anterior ostia) [kg s^-1]	4.01E-06	-1.61E-06
Mass flow rate (posterior ostia) [kg s^-1]	-4.00E-06	1.60E-06
Maximum velocity (anterior ostia) [m s^-1]	3.004e+00	9.523e-01
Maximum velocity (posterior ostia) [m s^-1]	1.979e+00	1.831e+00

Meanwhile during expiration in Fig. 6, the flow enters the sinus through the posterior ostium and exits at the anterior ostium. A small vorticity occurs at the posterior ostium. In Table I, the mass flow rate and maximum velocity that enters the sinus during inspiration is considerably high in comparison to that during expiration process.

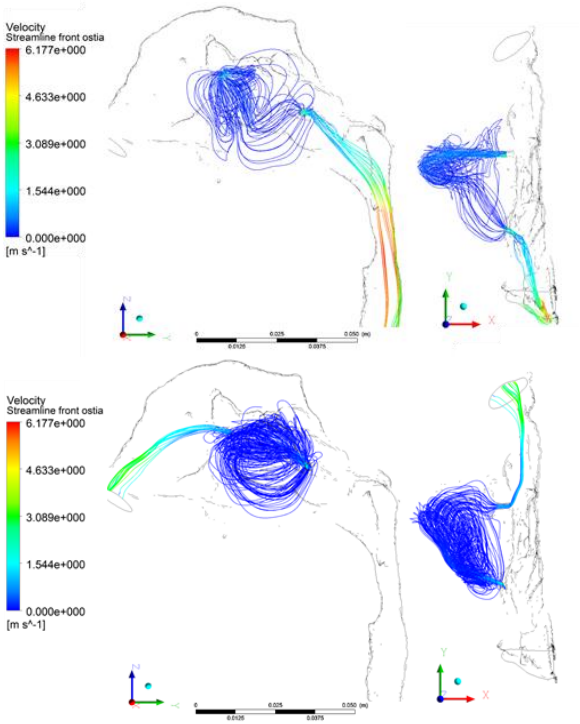

Figure 4. Streamlines in the sinus (side and top view) during inspiration (top) and expiration (bottom)

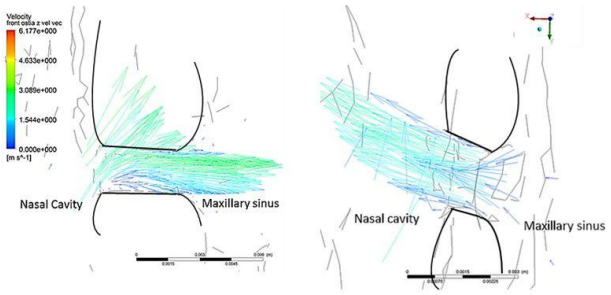

Figure 5. Velocity vectors in the anterior (left) and posterior (right) ostia at peak inspiration

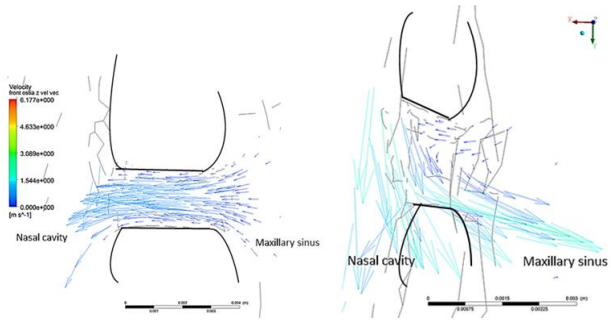

Figure 6. Velocity vectors in the anterior (left) and posterior (right) ostia at peak expiration

C. Presence of Anterior Ostium Only

With the presence of only anterior ostium, in Model C at peak inspiration, in view of velocity vectors of Fig. 7 the airflow generates a vortex with fairly high velocity at the ostium area, with nearly half of its velocity vectors going toward the sinus and the other half returning to the nasal cavity even before entering the sinus. In Fig. 8, the streamlines cannot be detected for the same velocity magnitude as in Model B. Meanwhile during expiration, a flow circulates at the entrance of the anterior ostia with very small tendency of going into the sinus.

Table II shows that, during inspiration, compared to previous model with both ostia (Model B), in model C, the mass flow rate entering the sinus is noticeably smaller in the anterior ostia and its maximum velocity is reduced by half, while during expiration, the entering mass flow rate is very little.

TABLE II. FLOW RESULTS IN MODEL C

Anterior ostia	Peak inhale	Peak exhale
Entering mass flow rate [kg s^-1]	6.17E-07	3.09E-09
Maximum velocity [m s^-1]	1.593e+00	1.051e-02

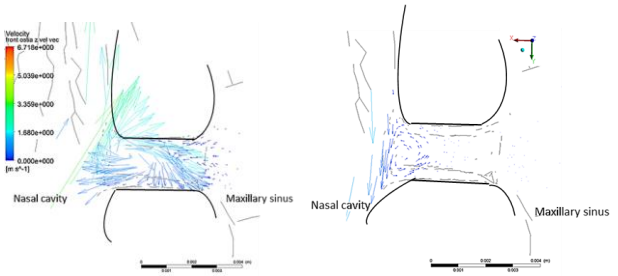

Figure 7. Velocity vectors in the anterior ostium only at peak inspiration (left) and expiration (right)

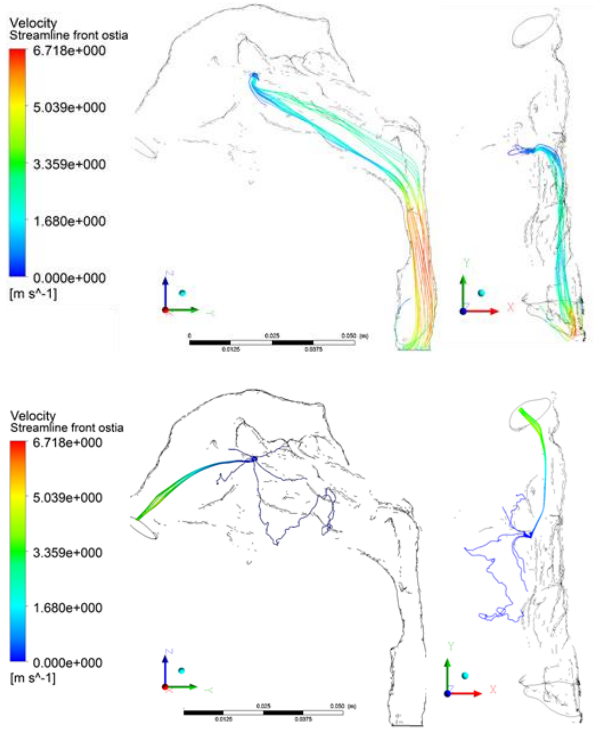

Figure 8. Streamlines in the sinus (side and top view) at peak inspiration (top) and expiration (bottom)

D. Presence of Posterior Ostium Only

From Fig. 9, during inspiration and expiration, a vortex can be observed at the ostium as the flow tends to flow into and out of the sinus. As shown in Fig. 10, although the flow circulation area detected in Model D is larger compared to Model C, it is smaller than in model B. As shown in Table III, unlike in the previous models, almost no discrepancy can be observed in both the entering mass flow rate and the maximum velocity between inspiration and expiration. Their order of magnitude in Model D is almost same to that at peak inhale of Model C

TABLE III. FLOW RESULTS IN MODEL D

Posterior ostia	Peak inhale	Peak exhale
Entering mass flow rate [kg s^-1]	3.72E-07	3.80E-07
Maximum flow velocity [m s^-1]	1.336e+00	9.767e-01

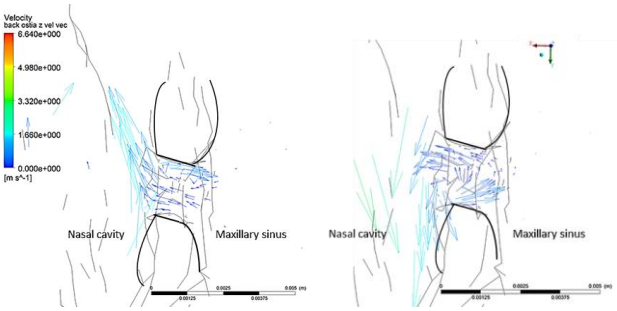

Figure 9. Velocity vectors in the posterior ostia only at peak inspiration (left) and expiration (right))

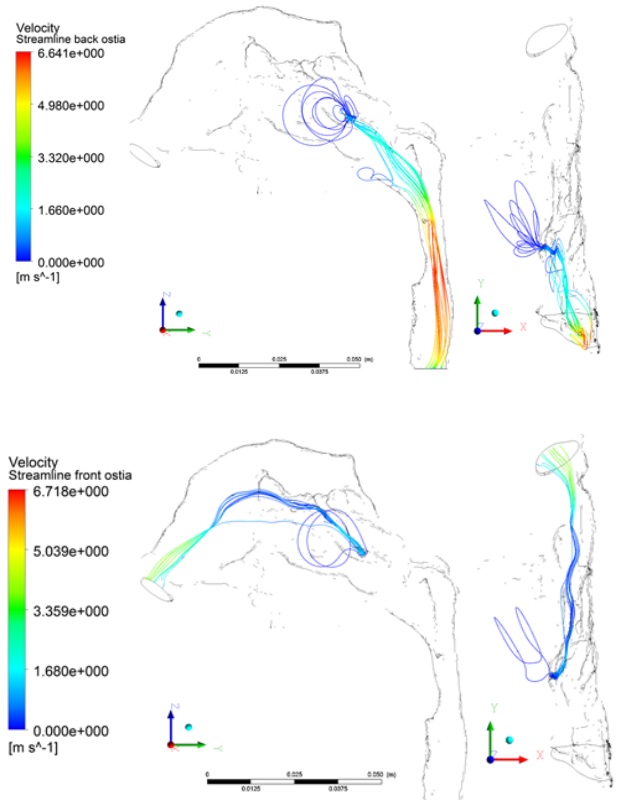

Figure 10. Streamlines in the sinus (side and top view) at peak inspiration (top) and expiration (bottom)

VI. Discussion

Almost no significant difference can be observed in the airflow pattern within the main nasal cavity Regardless of existence or non-existence of the maxillary sinus. This might be due to the small size of the ostia.

Regarding the distribution of streamlines, with the presence of both ostia in Model B, the flow circulated almost uniformly around the sinus during inspiration and expiration, on the contrary to the models with the existence of one ostium only.

In Models B and C, the entering mass flow rate at the entrance of the sinus (i.e., ostium) during inhalation is higher compared to that during exhalation. On the other hand, in Model D, the entering mass flow rate is almost same at inhalation and exhalation. The mass flow rate into or out of the sinus can be increased with the presence of multiple ostia in Model B as the flow enters and exits at different ostia, which is desirable for ventilation process. Meanwhile, with the existence of single ostium (anterior or posterior), a vortex appears in the ostium, which is in charge of flows into and out of the sinus at the same time.

VII. Conclusion

In this research, models of the maxillary sinus with variation of number and position of 2mm ostia were attached to the main nasal cavity.

As the results of flow patterns within the main nasal cavity, almost no significant difference can be observed between models with and without the presence of maxillary sinus. As mean diameter of ostia within a healthy person is about 2.4mm, extensive study on the variation of ostia diameter may contribute valuable information to this field.

Regarding flows in ostia and the sinus, the following results have been obtained:

(1) Mass flow rate into the sinus:
In the standard model with an anterior ostium only, the mass flow rate during inhalation is significantly higher in comparison to that during exhalation. The mass flow rate entering the sinus can be increased with the presence of multiple ostia as the flow enters and exits at different ostia. On the other hand in the model with a posterior ostium only, the mass flow rate is almost same at inhalation and exhalation.

(2) Flow patterns:
The flow patterns within the maxillary sinus changes with variation of number and location of ostia.

Further variation study is needed to clarify effects on the maxillary sinus physiology.

References

[1] E. Simon, "Anatomy of the opening of the maxillary sinus," *Arch Otolaryngol*, vol. 29, no. 4, pp. 640-649, 1939.

[2] M. Jog and G. W. McGarry, "How frequent are accessory sinus ostia?" *J Laryngol Otol*, vol. 117, no. 4, pp. 270-272, 2003.

[3] R. Aust and B. Drettner, "The functional size of the human maxillary ostium in vivo," *Acta Otolaryngology*, vol. 78, pp. 432-435, 1974.

[4] J. Ho-yeol, S. Seung-gul, P. Jae-bong, Hyoun-chull Kim., P. II-hae, and L. Sang-chull, "The change of maxillary sinus ostium in diameter following sinus floor elevation surgery using cone beam computered tomography," W. K. Chen, ed. in *Linear Networks and Systems*, Belmont, CA: Wadsworth, 1993, pp. 123-135.

[5] C. M. Hood, R. C. Schroter, D. J. Doorly, E. J. S. M. Blenke, and N. S. Tolley, "Computational modelling of flow and gas exchange in models of the human maxillary sinus," *J Appl Phsyiol*, vol. 107, no. 4, pp. 1195-1203, 2009.

[6] D. I. Hahn, P. W. Scherer, and M. M. Mozell, "Velocity profiles measured for air-flow through a large scale model of the human nasal cavity," *J Appl Physiol*, vol. 75, no. 5, pp. 2273-2287, 1993.

[7] D. F. Proctor and I. Andersen, "The nose: Upperway physiology and the atmospheric environment," *Amsterdam*: *Elseveir Biomedical*, 1982.

[8] Y. Izumi, T. Tajikawa, K. Ohba, and Y. Uesugi, "In vitro experiment on reciprocating flow in a model of the nasal cavities and pharynx," in *Proc. the 19th Bioengineering Conference, The Japan Society of Mechanical Engineers*, 2007.

Alias, Erny Afiza, she was born in Pahang, Malaysia on 4th January 1989. She attended twinning program between Malaysia and Japan (Japanese-associate degree in University Industry Selangor,UNISEL) and received her Degree in Mechanical engineering in 2011 from Tokai University. Soon as she has graduated, she pursued her study in Mechanical Engineering, majoring in fluid dynamics and obtained Master Degree in 2013. Currently, she is in the middle of her final year in PhD in the same field and major in Tokai University.

Yoko Takakura has her educational background here:
Doctor of Engineering, at Tohoku University, Japan, on July 1991,
Bachelor of Engineering, at the Department of Aeronautics and Astronautics, Faculty of Engineering, the University of Tokyo, Japan, on March 1979. She held the position professor at the Department of Prime Mover Engineering, Tokai University, 4-1-1, Kitakaname, Hiratsuka, Kanagawa 259-1292, Japan, from April 2014, Associate Professor at the above Institution, from April 2009, Assistant Professor at the Department of Mechanical Systems Engineering, Tokyo University of Agriculture and Technology, (Tokyo Noko University), Japan, from April 1994, Research Engineer at the Scientific Systems Department, Fujitsu Limited, Japan, from April 1979. During the above period, she experienced study abroad as a visiting scholar of JSPS (Japan Society for Promotion of Sciences) at Cambridge University, UK, from September 2000 to June 2001, Beijing University, Tsinghua University, China, September 1999. She has the publications belows
Fundamentals of Numerical Analysis —Algorithms and Errors —
(Tokyo, Japan: Corona Publishing Co., Ltd., 2007)
Articles:
Direct-Expansion Forms of ADER Schemes for Conservation Laws and Their Verifications, Journal of Computational Physics, Vol.219, No.2, Elsevier, pp.855-878, November 2006.
On TVD Difference Schemes for the Three-Dimensional Euler Equations in General Coordinates, International Journal for Numerical Methods in Fluids, Vol.9, No.8, John Wiley & Sons, pp.1011-1024, 1989.
Prof. Takakura is a member of
JSASS(Japan Society for Aeronautical and Space Sciences),
JSFM(Japan Society of Fluid Mechanics),
JSME(Japan Society of Mechanical Engineers),
JSAE(Japan Society of Automotive Engineers),
AIAA(American Institute of Aeronautics and Astronautcs),
She is awarded as
JSFM Fellow (from January 2008)
AIAA Associate Fellow (from January 2000)